

Journal Editorial Board

Editor-in-Chief

Robert Savinell

Case Western Reserve University
Cleveland, OH, USA

Technical Editors

Doron Aurbach

Bar-Ilan University
Ramat-Gan, Israel

Batteries and Energy Storage

David E. Cliffl

Vanderbilt University
Nashville, TN, USA

**Physical and Analytical Electrochemistry,
Electrocatalysis, and Photoelectrochemistry**

Gerald S. Frankel

The Ohio State University
Columbus, OH, USA

Corrosion Science and Technology

John Harb

Brigham Young University
Provo, UT, USA

Electrochemical Engineering

Takayuki Homma

Waseda University
Tokyo, Japan

Electrochemical/Electroless Deposition

Ajit Khosla

Yamagata University
Yamagata, Japan

Sensors

Janine Mauzeroll

McGill University
Montreal, QC, Canada

Organic and Bioelectrochemistry

Xiao-Dong Zhou

University of Louisiana at Lafayette
Lafayette, LA, USA

**Fuel Cells, Electrolyzers, and Energy
Conversion**

Associate Editors

Michael Adachi

Simon Fraser University, Canada

Brett Lucht

University of Rhode Island, USA

Rohan Akolkar

Case Western Reserve University, USA

Stephen Maldonado

University of Michigan, USA

Digital Repository Universitas Jember

Netz Arroyo

Johns Hopkins University School of Medicine,
USA

Scott Lillard

University of Akron, USA

Perla Balbuena

Texas A&M University

Thomas J. Schmidt

Paul Scherrer Institut, Switzerland

Thierry Brousse

University of Nantes, France

Minhua Shao

Hong Kong University of Science and Technology,
Hong Kong

Scott Donne

University of Newcastle, Australia

John A. Staser

Ohio University, USA

Olga Marina

Pacific Northwest National Laboratory, Richland, WA
USA

Alice Suroviec

Berry College, USA

Rajeev K. Gupta

North Carolina State University, USA

Thomas Thundat

University at Buffalo, USA

Charles L. Hussey

The University of Mississippi, USA

Nae-Lih (Nick) Wu

National Taiwan University, Taiwan

ECS Editorial Advisory Committee

Trisha Andrew (University of Massachusetts Amherst, USA)

S.V. Babu (Clarkson University, USA)

Lane Baker (Indiana University, USA)

Ronan Daly (University of Cambridge, UK)

Madhav Datta (Amrita School of Engineering, India)

Mike Hickner (Penn State University, USA)

Richard Keithley (Roanoke College, USA)

Sean King (Intel Corporation, USA)

Rainer Küngas (Haldor Topsøe A/S, Denmark)

Ramchandra Pode (Kyung Hee University, South Korea)

Anant Setlur (General Electric Global Research, USA)

Ryan West (University of San Francisco, USA)

Sheng-Joue Young (National United University, Taiwan)

Table of contents

Volume 168 Number 7, July 2021

1. Evaluation of Two-Electron Bispyridinylidene Anolytes and a TEMPO Catholyte for Non-Aqueous Redox Flow Batteries
Fahad Alkhayri and C. Adam Dyker
2. Facile Chemical Fabrication of a Three-Dimensional Copper Current Collector for Stable Lithium Metal Anodes
Shaobo Li, Qingquan He, Ke Chen, Shoushuang Huang, Fan Wu, Guiqiang Wang, Wangfei Sun, Shaqi Fu, Xiaoxiao Feng, Yue Zhou et al
3. Factors that Affect Capacity in the Low Voltage Kinetic Hindrance Region of Ni-Rich Positive Electrode Materials and Diffusion Measurements from a Reinvented Approach
Aaron Liu, Nutthaphon Phattharasupakun, Marc M. E. Cormier, Eniko Zsoldos, Ning Zhang, Erin Lyle, Phillip Arab, Montree Sawangphruk and J. R. Dahn
4. Understanding the Transport of Atmospheric Gases in Liquid Electrolytes for Lithium–Air Batteries
Ronja Haas, Michael Murat, Manuel Weiss, Jürgen Janek, Amir Natan and Daniel Schröder
5. Functional Gel Poly-m-phenyleneisophthalamide Nanofiber Separator Modified by Starch to Suppress Lithium Polysulfides and Facilitate Transportation of Lithium Ions for High-Performance Lithium-Sulfur Battery
Qi Yang, Chenzheng Yan, Xiaoxiao Wang, Hengying Xiang, Junyan Chen, Gang Wang, Liying Wei, Bowen Cheng, Nanping Deng, Yixia Zhao et al
6. Estimating the Diffusion Coefficient of Lithium in Graphite: Extremely Fast Charging and a Comparison of Data Analysis Techniques
Minkyu Kim, David C. Robertson, Dennis W. Dees, Koffi Pierre Yao, Wenquan Lu, Stephen E. Trask, Joel T. Kirner and Ira Bloom
7. Evidence for Li^+/H^+ Exchange during Ambient Storage of Ni-Rich Cathode Active Materials
Louis Hartmann, Daniel Pritzl, Hans Beyer and Hubert A. Gasteiger
8. Alkali Metal Ion Insertion and Extraction on Non-Graphitizable Carbon with Closed Pore Structures
Shota Tsujimoto, Yasuyuki Kondo, Yuko Yokoyama, Yuto Miyahara, Kohei Miyazaki and Takeshi Abe
9. The State of Health Estimation Framework for Lithium-Ion Batteries Based on Health Feature Extraction and Construction of Mixed Model
Qiaoni Han, Fan Jiang and Ze Cheng
10. Magnetic Control of Electrolyte Trapping Polysulfide for Enhanced Lithium-Sulfur Batteries
Yongan Cao, Qiao Wu, Yuchao Chen, Dong Chen, Chenlong Liu, Xiaoqian Hao, Tianjiao Zhu, Bo Zhang, Jiaxuan Zou and Wenju Wang
11. Enhanced Electrochemical Stability and Moisture Reactivity of Al_2S_3 Doped Argyrodite Solid Electrolyte

- Sanghyuk Min, Chanhwi Park, Insang Yoon, Gideok Kim, Kwonsoo Seol, Taeseung Kim and Dongwook Shin
12. Structural Modification of Negative Electrode for Zinc–Nickel Single–Flow Battery Based on Polarization Analysis
Shouguang Yao, Xinyu Huang, Xiaofei Sun, Rui Zhou and Jie Cheng
 13. A Sandwich Structure Composite Solid Electrolyte with Enhanced Interface Stability and Electrochemical Properties For Solid-state Lithium Batteries
Fei Chen, Jamans Luo, Mao-xiang Jing, Jie Li, Zhen-hao Huang, Hua Yang and Xiang-qian Shen
 14. Microfluidic Spinning of Core–Shell α -MnO₂@graphene Fibers with Porous Network Structure for All-Solid-State Flexible Supercapacitors
Yunming Jia, Xiaying Jiang, Arsalan Ahmed, Lan Zhou, Qinguo Fan and Shao Jianzhong
 15. An Initial Exploration of Coupled Transient Mechanical and Electrochemical Behaviors in Lithium Ion Batteries
Thomas Hodson, Shripad Patil and Daniel A. Steingart
 16. Polysulfide-Permanganate Flow Battery Using Abundant Active Materials
Zhiwei Yang, Michael R. Gerhardt, Michael Fortin, Christopher Shovlin, Adam Z. Weber, Mike L. Perry, Robert M. Darling and James D. Saraidaridis
 17. Modeling Studies of the Discharge Performance of Li-O₂ Batteries with Different Cathode Open Structures
Yuanhui Wang, Liang Hao and Minli Bai
 18. Investigation of Tetravalent Cation Doping with (M = Sn⁴⁺, Zr⁴⁺, and Ge⁴⁺) on the Electrochemical Properties of Monoclinic Li₃V₂(PO₄)₃ Using First-Principles Calculations
Chouaib Ahmani Ferdi, Mohammed Belaiche and Elabadila Iffer
 19. The Critical Role of Ionic Liquid Crystal on Mg²⁺ Ion Transport Properties in Magnesium Ion Batteries; Performance and Mechanism Approach
Nima Dalir, Soheila Javadian, S. M. Javad Ghavam and Hussein Gharibi
 20. An Artificial Interface for High Cell Voltage Aqueous-Based Electrochemical Capacitors
Marco Olarte, Marie-Joelle Menu, Patrice Simon, Marie Gressier and Pierre-Louis Taberna
 21. Oxygen Reduction/Evolution Activity of a Mechanochemically Synthesized Multilayer Graphene
Masayoshi Yuasa, Miu Tanaka, Masayo Shimizu and Mamia Yoshida
 22. Chemical Speciation of Zinc–Halide Complexes in Zinc/Bromine Flow Battery Electrolytes
Gobinath P. Rajarathnam, Thomas K. Ellis, Alexander P. Adams, Behdad Soltani, Renwu Zhou, Patrick J. Cullen and Anthony M. Vassallo
 23. An All-Aqueous Thermally Regenerative Ammonia Battery Chemistry Using Cu(I, II) Redox Reactions
Renaldo Springer, Nicholas R. Cross, Serguei N. Lvov, Bruce E. Logan, Christopher A. Gorski and Derek M. Hall
 24. Characterization of the Electrochemical Behavior of MnSO₄ with and without TiOSO₄ in H₂SO₄ Solution
Abdullah Omar O. Bahdad, Yuanchao Li and Trung Van Nguyen

25. Detection of Over-Discharged Nickel Cobalt Aluminum Oxide Lithium Ion Cells Using Electrochemical Impedance Spectroscopy and Differential Voltage Analysis
Norihiko Togasaki, Tokihiko Yokoshima and Tetsuya Osaka
26. Preparation of Current Collectors with Uniform Multi-Pits by Physical Rolling for Improving Full Battery Rate Performance
Jingrui Cao, Shiyu Tian, Kaicheng Zhang, Ruoxuan Liu, Hongyuan Guo, Lizhi Wen and Guangchuan Liang
27. Improved Low Temperature Performance of Graphite/Li Cells Using Isoxazole as a Novel Cosolvent in Electrolytes
Nuwanthi D. Rodrigo, Sha Tan, Zulipiya Shadike, Enyuan Hu, Xiao-Qing Yang and Brett L. Lucht
28. Bis(trifluoromethanesulfonyl)imide Metallic Salts Based Electrolytes for Electrochemical Capacitor Application: Theoretical vs Experimental Performance
T. Romann, J. Eskusson, T. Thomberg, E. Lust and A. Jänes
29. Enhanced Capacitive Performance of Mesoporous Vanadium Nitride Nanobelts
Zeyan Zhou, Zhao Liang, Gang Shao, Qiao Liu, Ding Chen and Weiyong Yang
30. Review—Recent Advances on High-Capacity Li Ion-Rich Layered Manganese Oxide Cathodes
Tumiso E. Mabokela, Assumpta C. Nwanya, Miranda M. Ndipingwi, Sinethemba Kaba, Precious Ekwere, Shane T. Werry, Chinwe O. Ikpo, Kwena D. Modibane and Emmanuel I. Iwuoha
31. Layered Vanadium Phosphates as Electrodes for Electrochemical Capacitors Part I: The Case of $\text{VOPO}_4 \cdot 2\text{H}_2\text{O}$
Jorge Alexis Zúñiga Martínez, Sara Elena González Nández, Etienne Le Calvez, Raúl Lucio Porto, Iván Eleazar Moreno Cortez, Thierry Brousse and Luis Alberto López Pavón
32. Implementation of a Physics-Based Model for Half-Cell Open-Circuit Potential and Full-Cell Open-Circuit Voltage Estimates: Part I. Processing Half-Cell Data
Dongliang Lu, M. Scott Trimboli, Guodong Fan, Ruigang Zhang and Gregory L. Plett
33. Implementation of a Physics-Based Model for Half-Cell Open-Circuit Potential and Full-Cell Open-Circuit Voltage Estimates: Part II. Processing Full-Cell Data
Dongliang Lu, M. Scott Trimboli, Guodong Fan, Ruigang Zhang and Gregory L. Plett
34. Pore Network Modelling of Galvanostatic Discharge Behaviour of Lithium-Ion Battery Cathodes
Zohaib Atiq Khan, Mehrez Agnaou, Mohammad Amin Sadeghi, Ali Elkamel and Jeff T Gostick
35. Intercalation of Lithium inside Bilayer Buckled Borophene: A First Principles Prospective
Muhammad Isa Khan, Sheeza Aslam, Abdul Majid and Syed Sajid Ali Gillani
36. Quantifying Negative Effects of Carbon-Binder Networks from Electrochemical Performance of Porous Li-Ion Electrodes
Aashutosh Mistry, Stephen Trask, Alison Dunlop, Gerald Jeka, Bryant Polzin, Partha P. Mukherjee and Venkat Srinivasan
37. Quantifying Uncertainty in Tortuosity Estimates for Porous Electrodes
Karthik S. Mayilvahanan, Zeyu Hui, Kedi Hu, Jason Kuang, Alison H. McCarthy, John Bernard, Lei Wang, Kenneth J. Takeuchi, Amy C. Marschilok, Esther S. Takeuchi et al

38. Energy-Dense Aqueous Carbon/Carbon Supercapacitor with a Wide Voltage Window
Janraj Naik Ramavath, Sravani Potham and Kothandaraman Ramanujam
39. Achieving High Stability and Rate Performance Using Spherical Nickel-Zinc Layered Double Hydroxide in Alkaline Solution
Runyue Qin, Yunpeng Pan, Zeang Duan, Huanhuan Su, Kailiang Ren, Wenfeng Wang, Yuan Li, Ning Xi, Yu Wang, Lu Zhang et al
40. High Capacity, Rate-Capability, and Power Delivery at High-Temperature by an Oxygen-Deficient Perovskite Oxide as Proton Insertion Anodes for Energy Storage Devices
Aman Bhardwaj, Hohan Bae, In-Ho Kim, Lakshya Mathur, Jun-Young Park and Sun-Ju Song
41. Improved Operando Raman Cell Configuration for Commercially-Sourced Electrodes in Alkali-Ion Batteries
Timothy E. Rosser, Edmund J. F. Dickinson, Rinaldo Raccichini, Katherine Hunter, Andrew D. Searle, Christopher M. Kavanagh, Peter J. Curran, Gareth Hinds, Juyeon Park and Andrew J. Wain
42. Enabling a Stable High-Power Lithium-Bromine Flow Battery Using Task-Specific Ionic Liquids
Supratim Das, Sahag Voskian, Krzysztof P. Rajczykowski, T. Alan Hatton and Martin Z. Bazant
43. Derivation of Transmission Line Model from the Concentrated Solution Theory (CST) for Porous Electrodes
Klemen Zelič, Tomaž Kutrašnik and Miran Gaberšček
44. Modeling of Lithium Intercalation in Twisted Bilayer Graphene
Victor Venturi and Venkatasubramanian Viswanathan
45. Deposition Behavior of Lead in Lead Methanesulfonate Flow Batteries with the Addition of Tin(II) Methanesulfonate
Zheng Liu, Jing Shi, Dongdong Ji, Xue Zhang and Bo Sun
46. Editors' Choice—Quantification of the Impact of Chemo-Mechanical Degradation on the Performance and Cycling Stability of NCM-Based Cathodes in Solid-State Li-Ion Batteries
Gioele Conforto, Raffael Ruess, Daniel Schröder, Enrico Trevisanello, Roberto Fantin, Felix H. Richter and Jürgen Janek
47. State of Charge Estimation of Battery Based on a New Equivalent Model
Fang Liu, Zhou Li, Wei-xing Su, Chang-ping Jiao and Yang Liu
48. Experiment and Simulation for Air-Cooling the Tabs of a Pouch Battery Module with Distributed Resistance Model
Haimin Wang, Si Chen, Zhiyuan Ji, Huanqi Li, Chenglong Jiang and Hao Lin
49. Electrochemical Performance of rGO@ZnCo₂O₄ Microspheres: Rationally Designed Asymmetric Constructed Wide-Potential Energy Storage Device
Meenu Sharma and Anurag Gaur
50. Compensation of the Irreversible Loss of Si-Anodes via Prelithiated NMC/LMO Blend Cathode
Nicola Michael Jobst, Giulio Gabrielli, Peter Axmann, Markus Hölzle and Margret Wohlfahrt-Mehrens

51. In-Situ Characterization for Solid Electrolyte Deformations in a Lithium Metal Solid-State Battery
Chuanwei Li, Siyuan Yang, Lipan Xin, Zhiyong Wang, Qiang Xu, Linan Li and Shibin Wang
52. Effect of Ni Content on Anionic Redox Activity in Ru-Containing Li-Rich Cathode Material
Kai Hu, Feng Zheng, Zi-Zhong Zhu and Shunqing Wu
53. Review—Recent Membranes for Vanadium Redox Flow Batteries
Baye Gueye Thiam and Sébastien Vaudreuil
54. Impact of Plasma and Thermal Treatment on the Long-term Performance of Vanadium Redox Flow Electrodes – Significance of Surface Structure vs Oxygen Functionalities
Tobias Greese, Paulette A. Loichet Torres, Davide Menga, Petra Dotzauer, Matthias Wiener and Gudrun Reichenauer
55. Effect of Electronic Conductivity on the Polarization Behavior of $\text{Li}[\text{Li}_{1/3}\text{Ti}_{5/3}]\text{O}_4$ Electrodes
Kingo Ariyoshi, Takaya Ino and Yusuke Yamada
56. First Principles Study of Oxygen Adsorption on Li-MO_2 ($M = \text{Mn}, \text{Ti}$ and V) (110) Surface
Khomotso P. Maenetja and Phuti E. Ngoepe
57. Operando Analysis of Interphase Dynamics in Anode-Free Solid-State Batteries with Sulfide Electrolytes
Andrew L. Davis, Eric Kazyak, Daniel W. Liao, Kevin N. Wood and Neil P. Dasgupta
58. Review—Clay Mineral Materials for Electrochemical Capacitance Application
Lun Zhang, Wei-Bin Zhang, Shan-Shan Chai, Xiong-Wei Han, Qiang Zhang, Xu Bao, Yao-Wen Guo, Xian-Li Zhang, Xia Zhou, Shao-Bo Guo et al
59. Increasing the Lithium Ion Mobility in Poly(Phosphazene)-Based Solid Polymer Electrolytes through Tailored Cation Doping
Tjark T. K. Ingber, Dominik Liebenau, Myra Biedermann, Martin Kolek, Diddo Diddens, Hans-Dieter Wiemhöfer, Andreas Heuer, Martin Winter and Peter Bieker
60. An Al-Cu Multielectrode Model for Studying Corrosion Inhibition with Praseodymium Mercaptoacetate at Intermetallic Particles in AA2024
R. A. Catubig, Y. J. Tan, A. E. Hughes, I. S. Cole, B. R. Hinton and M. Forsyth
61. Bulk Diffusion of Cl through O Vacancies in $\alpha\text{-Cr}_2\text{O}_3$: A Density Functional Theory Study
Kofi Oware Sarfo, O.Burkan Isgor, Melissa K. Santala, Julie D. Tucker and LÍney Árnadóttir
62. Enhanced Degradability of Mg-2Gd Alloy by Alloying Cu
Shiyu Zhong, Dingfei Zhang, Junyao Xu, Jie Zhou, Yang Zhao, Jingkai Feng, Yongqin Wang, Bin Jiang and Fusheng Pan
63. Passivation of Cu-Rh Alloys
Yusi Xie, Swarnendu Chatterjee, Ling-Zhi Liu, Hai-Jun Jin and Karl Sieradzki
64. The Effects of Perfluoroalkyl and Alkyl Backbone Chains, Spacers, and Anchor Groups on the Performance of Organic Compounds as Corrosion Inhibitors for Aluminum Investigated Using an Integrative Experimental-Modeling Approach
Milošev, A. Kokalj, M. Poberžnik, Ch. Carrière, D. Zimerl, J. Iskra, A. Nemes, D. Szabó, S. Zanna, A. Seyeux et al

65. Mechanistic Understanding of the Corrosion Behaviors of AZ31 Finished by Wire Electric Discharge Machining
Youmin Qiu, Lianxi Chen, Junjie Yang, Dahai Zeng, Hui Liu, Jiaping Han, Qi Li, Jianwei Li, Xiaohui Tu and Wei Li
66. Model Study of Penetration of Cl⁻ Ions from Solution into Organic Self-Assembled-Monolayer on Metal Substrate: Trends and Modeling Aspects
Anton Kokalj and Dominique Costa
67. Cathodic Kinetics on Platinum and Stainless Steel in NaOH Environments
R. M. Katona, J. Carpenter, E. J. Schindelholz, R. F. Schaller and R. G. Kelly
68. Al₂O₃ and HfO₂ Atomic Layers Deposited in Single and Multilayer Configurations on Titanium and on Stainless Steel for Biomedical Applications
Ivan Spajić, Ehsan Rahimi, Maria Lekka, Ruben Offoiach, Lorenzo Fedrizzi and Ingrid Milošev
69. Probing Barrier Oxide Layer of Porous Anodic Alumina by In Situ Electrochemical Impedance Spectroscopy
Alexey P. Leontiev and Kirill S. Napolskii
70. Communication—The Galvanic Effect on the Under-Deposit Corrosion of Titanium in Chloride Solutions
Y. Liu and E. Asselin
71. TiO₂ Nanotube Heterostructure Modified with a Metal-Organic Framework Showing Robust Stability for Photocathodic Protection
Xiayu Lu, Li Liu, Yu Cui and Fuhui Wang
72. Electrodeposition of Niobium from the CsBr-KBr-NbBr₃ Melt
Alexander Chernyshev, Alexey Apisarov, Alexander Shmygalev, Pavel Pershin, Alexander Kosov, Olga Grishenkova, Andrey Isakov and Yury Zaikov
73. Studies on Direct Electrochemical De-Oxidation of Solid ThO₂ in Calcium Chloride Based Melts
Anwasha Mukherjee, Kumaresan R. and Kitheri Joseph
74. Hard Magnetic Properties of Nanocrystalline Cobalt-Phosphorus (Co₁₀₀-XPX) Electrodeposits
Dung T. To, Doek-Yong Park, Bongyoung Yoo, Saba Seyedmahmoudbaraghani, Sun Hwa Park and Nosang V. Myung
75. Operando Laser Scattering: Probing the Evolution of Local pH Changes on Complex Electrode Architectures
Vitali Grozovski, Pavel Moreno-García, Elea Karst, María de Jesús Gálvez-Vázquez, Alexander Fluegel, Sathana Kitayaporn, Soma Vesztergom and Peter Broekmann
76. In Situ Surface Roughness Analysis of Electrodeposited Co Films in an Ionic Liquid Using Electrochemical Surface Plasmon Resonance: Effect of Leveling Additives
Naoya Nishi, Kenta Ezawa and Tetsuo Sakka
77. Electrochemical Behavior of PdCl₂ in 1-Ethyl-3-Methylimidazolium Chloride Ionic Liquid at Pt-Ir Electrode
Wu Zhang and Batric Pesic
78. Crossover between Re-Nucleation and Dendritic Growth in Electrodeposition without Supporting Electrolyte
Chams Kharbachi, Théo Tzedakis and Fabien Chauvet

79. Enhanced Thermoelectric Properties of Skutterudite Thick Film Polyvinyl Alcohol Assisted from the Post-Deposition Annealing Effect
Nuur Syahidah Sabran, Iman Aris Fadzallah, Mohd Faizul Mohd Sabri, Takahito Ono, Khairul Fadzli Samat, Siti Nor Farhana Yusuf and Rahman Saidur
80. Investigation of Pulse Electrochemical Machining of Zr-Based Bulk Metallic Glasses in NaNO₃-Ethylene Glycol Electrolyte
Cheng Guo, Bo Wu, Bin Xu, Shiyun Wu, Jun Shen and Xiaoyu Wu
81. Chronopotentiometric Study and Morphological-Structural Characterization of Environmentally Friendly Protective Zn-Mn Coatings
N. Loukil and M. Feki
82. Obtaining High Surface Quality in Electrochemical Machining of TC17 Titanium Alloy and Inconel 718 with High Current Densities in NaNO₃ Solution
Yudi Wang, Zhengyang Xu, Deman Meng and Zhen Wang
83. Study of Preventing the Alumina Dissolution and Metal Ion Migration in the Ceramic Membrane Divided-Electrochemical Cell Worked with High Acid-Base Electrolyte
P. Silambarasan and I. S. Moon
84. Alkaline Electrochemical Reduction of a Magnesium Ferrosphalite into Metallic Iron for the Valorisation of Magnetite-Based Metallurgical Waste
Daniela V. Lopes, Aleksey D. Lisenkov, Sergii A. Sergiienko, Gabriel Constantinescu, Artur Sarabando, Margarida J. Quina, Jorge R. Frade and Andrei V. Kovalevsky
85. Critical Parameter Identification of Fuel-Cell Models Using Sensitivity Analysis
Lalit M. Pant, Sarah Stewart, Nathan Craig and Adam Z. Weber
86. Analytical Warburg Impedance Model for EIS Analysis of the Gas Diffusion Layer with Oxygen Depletion in the Air Channel of a PEMFC
Samuel Cruz-Manzo and Paul Greenwood
87. Method—Practices and Pitfalls in Voltage Breakdown Analysis of Electrochemical Energy-Conversion Systems
Michael R. Gerhardt, Lalit M. Pant, Justin C. Bui, Andrew R. Crothers, Victoria M. Ehlinger, Julie C. Fornaciari, Jiangjin Liu and Adam Z. Weber
88. Simulative Investigation on Local Hydrogen Starvation in PEMFCs: Influence of Water Transport and Humidity Conditions
Fengmin Du, Julian Arndt Hirschfeld, Xinyi Huang, Krzysztof Jozwiak, Tuan Anh Dao, Andreas Bauer, Thomas J. Schmidt and Alin Orfanidi
89. Effects of Gas Diffusion Layer Substrates on PEMFC Water Management: Part I. Operando Liquid Water Saturation and Gas Diffusion Properties
Hong Xu, Minna Bührer, Federica Marone, Thomas J. Schmidt, Felix N. Büchi and Jens Eller
90. Impact of Surface Hydrophilicity of Gas-Diffusion-Type Biocathodes on Their Oxygen Reduction Ability for Biofuel Cells
Ryoichi Tatara, Shun Sakai, Tatsuo Horiba and Shinichi Komaba
91. The Impact of Micro Porous Layer on Liquid Water Evolution inside PEMFC using Lattice Boltzmann Method
92. M. Sepe, P. Satjaritanun, I. V. Zenyuk, N. Tippayawong and S. Shimpalee
93. Electrochemical Oxidation of 2,3-Dihydroxypyridine in the Presence of Benzenesulfonic Acid: A Green Method for the Synthesis of a Novel Heterocycle Dye
Hamed Goljani, Zahra Tavakkoli and Davood Nematollahi

94. Electroreduction of Acetochlor at Silver Cathodes in Aqueous Media
Ana G. Couto Petro, Nicholas F. Scherschel and Lane A. Baker
95. Review—Electrochemical Strategies for Selective Fluorination of Organic Compounds
Ditto Abraham Thadathil, Anitha Varghese and Kokkuvayil Vasu Radhakrishnan
96. The Critical Role of the Solvent Effect on Titanium Anodizing Current
Qinyi Zhou, Qianqian Liu, Ancheng Wang, Shuang Chen, Wenchao Zhang, Ye Song and Xufei Zhu
97. Amorphous Nickel Oxide as Efficient Electrocatalyst for Urea Oxidation Reaction
Qingqing Wang, Yongdan Li and Cuijuan Zhang
98. Evaluation of Ni₀, NiO, and NiS as a Cocatalyst Modifier on TiO₂ Nanotubes Matrix for the Enhancement of Photoelectrocatalytic Oxidation of Penicillin G
Fabiana Avolio Sayão, Alysson Stefan Martins, Josiel José da Silva and Maria Valnice Boldrin Zanoni
99. A Self-Standing 3D Heterostructured N-Doped Co₄S₃/Ni₃S₂/NF for High-Performance Overall Water Splitting
Han Jiang, Huiting Yuan, Liguang Zhang, Wenjun Dong, Yueqi Chang, Xilai Jia and Ge Wang
100. Kinetics of Oxidation of Reduced Forms of Adsorbed CO₂ on a (pc)Pt Electrode in Saturated H₂CO₃ under Quasi-Equilibrium Conditions: The Effect of the Potential Oscillations
Alexander V. Smolin, Aleksey F. Gadzaov and Leonid M. Kustov
101. Effect of Triton X-100 on the Electrochemical Behavior of Hydrophobic Lapatinib Used in the Treatment of Breast Cancer: A First Electroanalytical Study
Begum Evranos Aksoz and Burcu Dogan Topal
102. Impact of pH on the Anodic Current-Voltage Characteristics of the Alkaline Cu | Cu (II), Glycine System
Arvydas Survila, Stasė Kanapeckaitė, Olga Girčienė and Laima Gudavičiūtė
103. Electrodeposition Behavior of Extracted Platinum Complex in Phosphonium-Based Ionic Liquids Evaluated by Electrochemical Quartz Crystal Microbalance
Masahiko Matsumiya, Yusuke Tsuchida, Ryoma Kinoshita and Yuji Sasaki
104. An Innovative Sensor Construction Strategy via LbL Assembly for the Detection of H₂O₂ Based on the Sequential In Situ Growth of Prussian Blue Nanoparticles in CMC-PANI Composite Film
Sinan Uzunçar, Nizamettin Ozdogan and Metin Ak
105. The Effect of Mo Addition on Electrocatalytic Activity and Stability of Fe-Co-P-C Metallic Glasses for Hydrogen Evolution
Fabao Zhang, Wenbing Shan, Qingzhuo Hu, Wei Jiang, Dongdong Li and Bo Zhang
106. Design of an Electrochemical Sensor Using 2D Sheet-Like Cu@g-C₃N₄ Transducer Matrix for Electroanalysis of Catechol
Ballur Prasanna Sanjay, Ningappa Kumara Swamy, Shivamurthy Ravindra Yashas and Shadakshari Sandeep
107. Electrochemical Oscillations (Named Oscillations H and K) during H₂O₂ Reduction on Pt Electrodes Induced by a Local pH Increase at the Electrode Surface
Haruki Okada, Ryusuke Mizuochi, Yuri Sakurada, Shuji Nakanishi and Yoshiharu Mukouyama

108. A PCR-Free Genome Detection of Mycobacterium Tuberculosis Complex in Clinical Samples using MWCNT/PPy/KHApNps Modified Electrochemical Nano-Biosensor
Kobra Salimiyan Rizi, Zahra Meshkat, Mohammad Chahkandi, Mehrdad Gholami, Mojtaba Sankian, Kiarash Ghazvini, Hadi Farsiani, Ehsan Aryan and Majid Rezayi
109. Communication—An Optical Fiber Biosensor Based on a Lab-on-a-Tip Approach for User-Friendly Carbosulfan Detection in Vegetable Samples
B. Kuswandi, M. R. Taufikurrohman and A. S. Nugraha
110. Engineering Layered Nanostructures of Two-Dimensional Transition Metal Dichalcogenides with CeO₂ for Nano-Level Detection of Promethazine Hydrochloride
Subash Vetri Selvi, Nandini Nataraj, Tse-Wei Chen, Shen Ming Chen, Wei-Ling Wu, Tien-Wen Tseng and Chih-Ching Huang
111. Nipping the Shape of the Nanosilver through Bio-Based Capping Strategy and Studies on Their Electrocatalytic Performance Using Electro Spectrometry
S. Sivakala, E. Rishad Baig, C. Molji, Aravind Aashish, Asha S. Kumar and Sudha J. Devaki
112. The Real Current Density Distribution on Mg Surface
Jufeng Huang, Guang-Ling Song, Ziming Wang and Dajiang Zheng
113. Direct Detection of Ofloxacin using MWCNT@Sm(OH)₃ Nanocomposite Modified Carbon Paste Electrode
Mehrnaz Ebrahimi, Mahya Ghorbani, Parviz Norouzi and Ehsan Ghods Rad
114. A La₂O₃ Nanoparticle SO₂ Gas Sensor that Uses a ZnO Thin Film and Au Adsorption
Ting-Jen Hsueh and Shih-Hsien Lee
115. Review—Recent Progress in the Diversity of Inkjet-Printed Flexible Sensor Structures in Biomedical Engineering Applications
Hanim Hussin, Norhayati Soin, Sharifah Fatmadiana Wan Muhamad Hatta, Fazliyatul Azwa Md Rezali and Yasmin Abdul Wahab
116. Synthesis of Novel Iron Porphyrin/Titanoniobate Nanocomposite for Electrochemical Detection of Uric Acid
Haoran Wang, Tongtong Cao, Shining Wu, Shengkang Wang, Changyong Yan, Zhengjun Wang, Xiaobo Zhang and Zhiwei Tong
117. Rapid and Label-Free Electrochemical Detection of Fumonisin-B1 Using Microfluidic Biosensing Platform Based on Ag-CeO₂ Nanocomposite
Tarun Kumar Dhiman, G. B. V. S. Lakshmi, Kashyap Dave, Appan Roychoudhury, Nishu Dalal, Sandeep K. Jha, Anil Kumar, Ki-Ho Han and Pratima R. Solanki
118. Non-Enzymatic Methyl Parathion Electrochemical Sensor Based on Hydroxyl Functionalized Ionic Liquid/Zeolitic Imidazolate Framework Composites Modified Glassy Carbon Electrode
Yutong Li, Chao Du, Xinsheng Liu, Kai Wang, Huifang Yang and Yonghong Li
119. Molecularly Imprinted Scaffold Based on poly (3-aminobenzoic acid) for Electrochemical Sensing of Vitamin B6
Anila Rose Cherian, Libina Benny, Anitha Varghese, Neena S. John and Gurumurthy Hegde
120. Pico Molar Sensing of Dopamine in Presence of Serotonin Using BaMnO₃/Carbon Nanostructures
Jasmine Thomas, P. K. Anitha, Tony Thomas and Nygil Thomas

121. Evaluation of Permselective Polydopamine/rGO Electrodeposited Composite Films for Simultaneous Voltammetric Determination of Acetaminophen and Dopamine
Fang Xie, Yueming Zhou, Xizhen Liang, Kanglin Wu, Zhiyi Zhou, Mingshi Bao, Jinsong Zhang, Jianqiang Luo, Shujuan Liu and Jianguo Ma
122. A Neoteric Double Perovskite Gd_2NiMnO_6 Nanostructure Electrocatalyst for Augmented Detection of Ecological Pollutant 2, 4, 6 Trichlorophenol
Subburaj Srinithi, Praveen Kumar Gopi, Tse-Wei Chen, Shen-ming Chen, Ramaraj Sayee Kannan, Nora Hamad Al-Shaalan, Mohamed Ouladsmame, Mohammad Ajmal Ali and Xiaoheng Liu
123. High-Performance Electrochemical Sensor Based on Yttrium Sulfide Nanoparticles Decorated Carbon Nitride Heterostructure for Highly Sensitive Detection of Antimicrobial Drug in Biological Samples
Kumar Gokulkumar, Ashok K. Sundramoorthy, Sea-Fue Wang, A. Harikrishnan and Razan A. Alshgari
124. ZIF-L Derived Bimetallic N-Doped Porous Carbon-Prussian Blue Composite as Efficient Catechol Electrochemical Sensor
Ziyu Zhao, Jialun Luo, Simon Tricard, Jihua Zhao, Qiangming Wang and Jian Fang
125. Biosensor Encapsulation via Photoinitiated Chemical Vapor Deposition (piCVD)
Ruolan Fan and Trisha L. Andrew
126. An Odor Recognition Algorithm of Electronic Noses Based on Convolutional Spiking Neural Network for Spoiled Food Identification
Yizhou Xiong, Yuantao Chen, Changming Chen, Xinwei Wei, Yingying Xue, Hao Wan and Ping Wang
127. Synthesis and Application of Graphdiyne Oxide-Polyurethane Nanocomposite Yield a Highly Sensitive Non-Enzyme Glucose Sensor
Chakavak Esmaeili, Jin Song, Yuliang Li, Lanqun Mao, Huibiao Liu, Fei Wu, Yanhuan Chen, Chenli Liu and Xian-En Zhang
128. Molecularly Imprinted Electrochemical Sensor Based on 3D Wormlike PEDOT-PPy Polymer for the Sensitive Determination of Rutin in Flos Sophorae Immaturus
Rongqian Meng, Jianke Tang, Xiaojun Wu, Shengjian Zhang, Xin Wang, Qiaoling Li and Riya Jin
129. Erratum—Redox Potential Measurements of Cr(II)/Cr Ni(II)/Ni and Mg(II)/Mg in Molten $MgCl_2$ -KCl-NaCl Mixture [J. Electrochemi Soc., 167, 116505 (2020)]
Mingyang Zhang, Jianbang Ge, Taiqi Yin and Jinsuo Zhang
130. Erratum: Electrochemical Performance of Sol-Gel Synthesized $NaTi_2(PO_4)_3$ -Carbon Composites as Aqueous Na-ion Battery Anodes [J. Electrochem Soc., 168, 060545 (2021)]
Skirmantė Tutlienė, Milda Petrulėvičienė, Jurgis Pilipavičius, Aleksej Žarkov, Algirdas Selskis, Sandra Stanionytė, Jurga Juodkazytė and Linas Vilčiauskas
131. Erratum: Evaluation of Heat Generation and Thermal Degradation of Lithium Ion Batteries by a Calorimetry Method [J. Electrochem. Soc., 168, 060553 (2021)]
Ya Mao, Rui Guo, Liangmei Sheng, Shangde Ma, Luozeng Zhou, Liqin Yan, Chen Yang and Jing-Ying Xie
132. Erratum: Passivation of Cu-Rh Alloys [J. Electrochem. Soc., 168, 071505 (2021)]
Yusi Xie, Swarnendu Chatterjee, Ling-Zhi Liu, Hai-Jun Jin and Karl Sieradzki

OPEN ACCESS

Communication—An Optical Fiber Biosensor Based on a Lab-on-a-Tip Approach for User-Friendly Carbosulfan Detection in Vegetable Samples


To cite this article: B. Kuswandi *et al* 2021 *J. Electrochem. Soc.* **168** 077502

View the [article online](#) for updates and enhancements.





Communication—An Optical Fiber Biosensor Based on a Lab-on-a-Tip Approach for User-Friendly Carbosulfan Detection in Vegetable Samples

B. Kuswandi,^z  M. R. Taufikurrohman, and A. S. Nugraha

Chemo and Biosensors Group, Faculty of Pharmacy, University of Jember, Jember, 68121, Indonesia

The use of a disposable pipette tip was studied to create a lab-on-a-tip approach. The configuration of a pipette tip, fiber optics, and paper-based biosensor show the compatibility of creating a novel one-shot optical biosensor for carbosulfan as carbamate pesticide. Under optimal experimental parameters, the lab-on-a-tip could detect carbosulfan in the linear range value of 10–22000 $\mu\text{g l}^{-1}$ with a detection limit value of 10 $\mu\text{g l}^{-1}$. The results show good agreement with the HPLC method.

© 2021 The Author(s). Published on behalf of The Electrochemical Society by IOP Publishing Limited. This is an open access article distributed under the terms of the Creative Commons Attribution 4.0 License (CC BY, <http://creativecommons.org/licenses/by/4.0/>), which permits unrestricted reuse of the work in any medium, provided the original work is properly cited. [DOI: 10.1149/1945-7111/ac0ec2]



Manuscript submitted January 31, 2021; revised manuscript received June 5, 2021. Published July 5, 2021.

The search for new materials or platforms to be integrated into sensing design and devices is an interesting topic in sensor development, particularly a user-friendly and integrated device that no need for sample treatment and expertise. For this purpose, a pipette tip can be used as a novel approach in sensor development. For example, a pipette tip was developed as a pool optode for Hg (II) ions sensing.¹ A pipette tip containing amine-functionalized sol-gel to enrich and purify phosphopeptides called a “lab-in-a-pipet-tip” was employed for mass spectroscopy measurements.² Furthermore, a pipette tip was used as a lab-on-a-tip to create an electroanalysis system for Cu(II) ions detection.³ Here, a pipette tip can provide a sensing system for field application. Furthermore, it can be combined with other materials, such as paper and cotton. Generally, like lab on a chip (LOC),^{4,5} lab-on-a-tip (LOT) can be presented as a sensing platform where one or several tools integrated on a miniaturized single tip,⁶ and detection can be done by electrical, optical, or mechanical techniques. However, LOT is in infancy and typically developed for a single analyte, but its potential to be developed for multiple analytes is promising that can be integrated with imaging, diagnostics, and therapeutic function.⁶

In the case of a paper-based sensor, it allows providing portable devices that are simple, flexible, and low-cost.⁷ This low-cost technology employs hydrophilic paper to create hydrophobic channels by patterning.⁸ It is introduced to the device to examine a sample solution and flowed through a sensing zone by capillary without external power.^{9,10} Among these techniques, the most widely used is colorimetric detection. Since a color change can be detected via ligand-analyte interaction.^{11,12} The main advantages of the paper platform are (i) adsorption properties; (ii) capillary action; (iii) high surface to volume ratio; (iv) suitable with various samples; (v) allow immobilization of biomolecules (e.g., enzyme, proteins, and antibodies),^{13,14} very light and readily available.¹⁵ Moreover, paper allows to transport and absorption of reagents within its substrate, without the need for reagents handling, and simple disposal by incineration, and simple fabrication (e.g., wax printing) at a low-cost.¹⁶

In this work, we propose a novel concept in fiber optic sensors employing a pipette tip, by adopting as the optical cell, where the paper-based biosensors attached inside a tip wall to perform optical detections via optical fiber. The LOT is highly portable, and allowing both to load a sample and to react with the biosensor inside the tip, and provides the user a laboratory system. Furthermore, it allows using very low sample volume to be detected,

reducing the waste that is often produced in the automatic detection, such as flow analysis.^{17,18} Herein, the carbosulfan as carbamate pesticides were selected as an analyte. Compared to the other optical biosensors for pesticides, such as biosensor based on the recovered fluorescence of carbon dots-Cu(II) system,¹⁹ lab-on-a-drop,²⁰ colorimetric and phosphomimetic dual signaling strategy,²¹ and GQDs-MnO₂ based assay with turn-on fluorescence,²² this approach offers simple and user-friendly pesticide detection in real samples, such as vegetable samples. Moreover, it can easily be suited to other platforms (e.g., polymeric membrane), other analytes, or different sensing techniques, such as electrochemical³ or mechanical techniques.⁶

Experimental

Paper-based biosensor fabrication.—The paper-based biosensor was fabricated using filter paper (Whatman, cat no 1001–150) and shaped into a circle paper (7 mm diameter). The paper was then impregnated with polyvinyl alcohol (1%) for overnight to increase the bonding of paper with enzyme and reagent used, and to enhance enzyme activity in the immobilized phase.^{23,24} Afterward; the impregnated paper was completely dried at room temperature. The paper was then firstly immobilized with 2 μl acetylcholinesterase/AchE (EC. 3.1.1.7, Electrophorus electricus, 518 IU mg^{-1} solid, 1 mg AchE in 1 ml tris-buffer 7.5 mM, at pH 7.5), and left for dry at room temperature (25 °C). Secondly, 2 μl bromothymol blue (6000 mg l^{-1} at ethanol-water mixture (25% v/v)) was immobilized on the enzyme-paper to create a paper-based biosensor. After the biosensor was completely dried at room temperature (25 °C), it was ready to be integrated into the LOT or stored in chiller condition (~ 4 °C) for further use.

LOT set-up.—The experimental set-up consists of a pipette tip (100- μl plastic tips) containing a paper-based biosensor and micro-pipette (10–100- μl , Socorex, Germany). A circle piece of the paper-based biosensor (7 mm) was attached inside the pipette wall using double tape (Fig. 1A). Afterward, the sample was loaded into the tip and direct detected with the biosensor. This procedure allowed for sample delivery and detection of an analyte with increased reproducibility as the sample volume loaded in the fixed volume and fixed position when the analyte interacts with the biosensor membrane.

The reflectance measurements were acquired in the visible wavelength between 400–800 nm using a fiber optic portable spectrometer (USB 2000, Ocean Optic, USA). The inhibition measurement of carbosulfan was carried out by calculating the reflected intensity response according to Eq. 1. For simple measurement, the LOT was employed as a disposable, as it does not need for regeneration of the inhibited enzyme in this case. Moreover, the

^zE-mail: b_kuswandi.farmasi@unej.ac.id

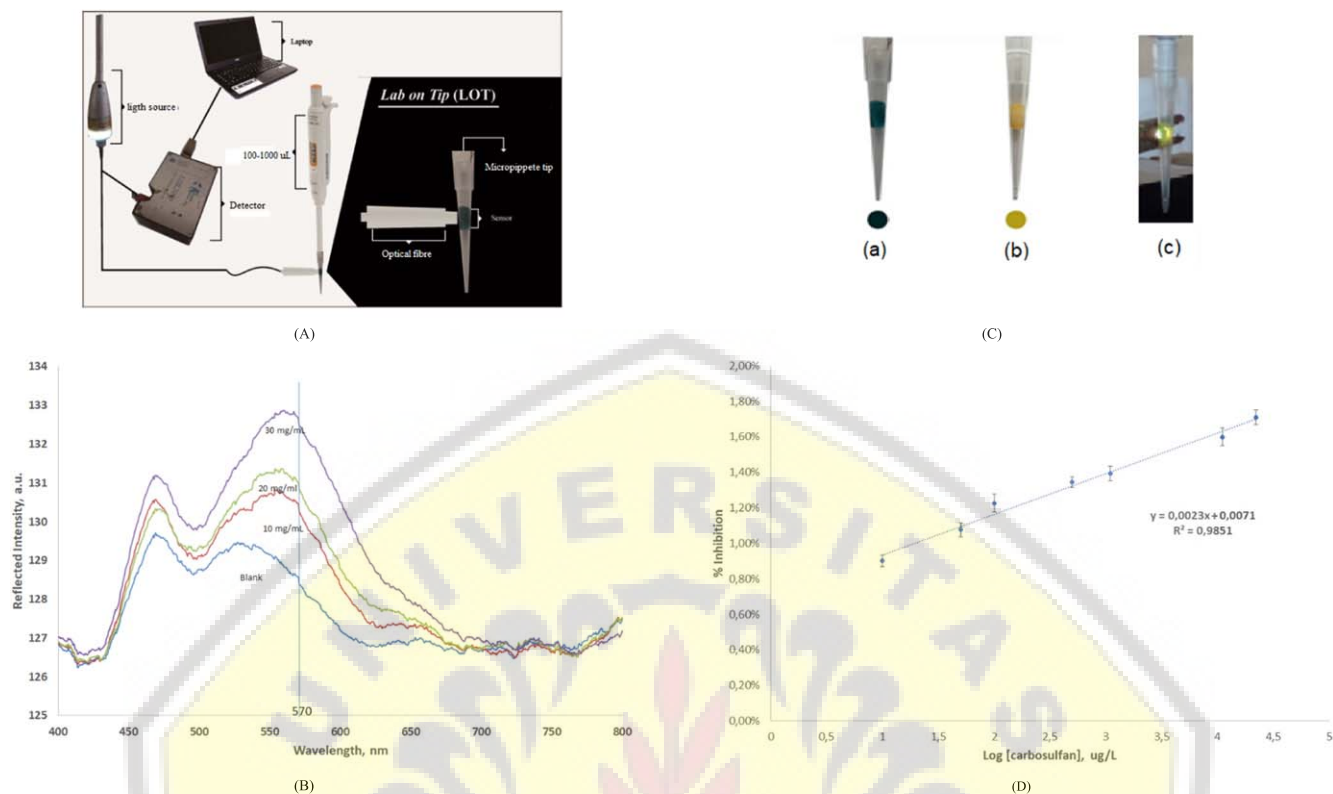


Figure 1. (A) The LOT set-up for carbosulfan detection in food samples. (B) The spectra of LOT toward the substrate (acetylcholine), where the maximum wavelength was at 570 nm. (C) the color change of the paper-based biosensor, before (a) and after reaction with a substrate (b), and under fiber optic light (c). (D) Calibration curve of the carbosulfan concentrations ($10\text{--}220 \mu\text{g l}^{-1}$) vs % inhibition performed by LOT biosensor.

transparent plastic tip helped in the detection of the color change of the biosensor inside the LOT by a nude eye.

Inhibition measurement.—Initially, $100 \mu\text{l}$ of the substrate (ACh) at a tris-buffer solution (pH 7.5) was loaded into the LOT to determine the enzyme initial activity, i.e., absence of inhibition (E_o), and drained out. The carbosulfan solution ($100 \mu\text{l}$) was loaded into the LOT. After optimized inhibition time, the sample solution was drained out, and the residual enzyme activity was obtained by a substrate (ACh) loaded into the LOT, and the percentage inhibition (%I) was calculated according to the following equation:

$$\text{Inhibition}(\%I) = (E_o - E_i)/E_o \times 100\% \quad [1]$$

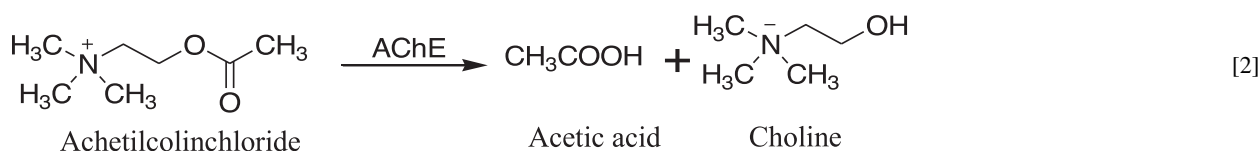
where E_o and E_i are the reflected signal intensity for substrate and inhibitor plus substrate, respectively.

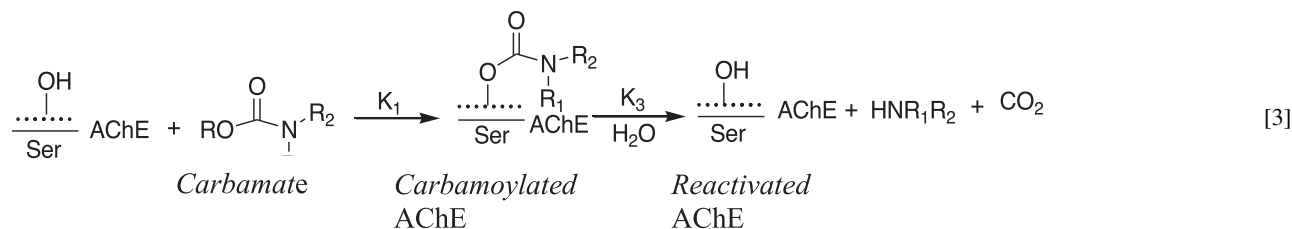
Real sample preparation.—The vegetable samples (lettuce, cabbage, and tomato) and rice samples (organic and non-organic rice) were collected from the traditional market at Jember-Indonesia. Each sample was prepared according to Kuswandi et al.,²⁵ with slight modification. The sample was crushed using a mortar and a sample portion (0.5 g) was taken for pesticide extraction. Then distillate water was added to the sample until the volume was 10 ml. Afterward, the mixture was ultrasonicated for 15 min followed by centrifugation at 3000 rpm for 15 min. The filtrate was taken for

carbosulfan detection using the LOT. While for HPLC protocol, the crushed sample (0.5 g) was added with methanol until the volume was 10 ml. Then, the solution mixture was ultrasonicated for 15 min, then centrifuged at 3000 rpm for 15 min. The filtrate obtained needs to be filtered by the filter membrane (PTFE, 47 mm, pore size $0.20 \mu\text{m}$, Shimadzu, Japan) before it can be injected into an HPLC system.²⁶ Shimadzu HPLC system used consist of SPD 20 A UV-vis detector, an LC 20AD isocratic pump, and a C18 column ($4.6 \times 250 \text{ mm}$, $4 \mu\text{m}$, 100 \AA), controlled by LC software.

Results and Discussion

The biosensing scheme obtaining from a paper-based biosensor towards carbosulfan can be described below. In the uninhibited biosensor, a pH change caused by the acetic acid produced during the enzymatic reaction as given in Eq. 2 was measured as the blank signal. While the inhibited biosensor, a pH change is inhibited by carbosulfan, was measured as the inhibited signal. As a complete pesticide detection, a net of pH change before and after inhibition of the AchE was calculated. Here, the AchE inhibition corresponds to the acylation of the serine-OH in the AchE active site by pesticides.^{25,27} The biosensing scheme using AchE is similar to the enzyme-substrate reaction, whereby a Michaelis enzyme-pesticide complex is first formed, then followed by the transfer of the pesticide acyl groups to the serine-OH of the enzyme, along with the side product (HNR_1R_2) release.²⁷ Thus, the AchE inhibition by carbosulfan is presented as Eq. 3:





According to the scheme, to create the sensitive biosensor response toward carbosulfan, the paper-based biosensor needs to be well constructed, including acetylcholine used as a substrate, the maximum wavelength used for the reflectance measurement, and inhibition time used in the LOT need to be optimized. Using various substrate concentrations, the spectra measurements were performed. According to Fig. 1B, the maximum wavelength was found at 570 nm. To select optimum substrate for biosensing process via enzymatic reaction, the various concentration of acetylcholine was tested in the range 10,000–50,000 $\mu\text{g ml}^{-1}$, where the substrate concentration was optimum at 40,000 $\mu\text{g ml}^{-1}$. Moreover, this color change could also be detected visually by the naked eye (Fig. 1C), so it is open-up for using another detection, such as colorimetric analysis using a smartphone via the App. (e.g., imageJ,²⁸ and color grab²⁹). To detect a very low concentration of carbosulfan as an inhibitor, the low carbosulfan residue (100 $\mu\text{g l}^{-1}$) was tested. Here, the inhibition time was tested between 5–25 min, and 15 min was found to be optimum.

In order to detect carbosulfan at trace concentration ($\mu\text{g l}^{-1}$ or ppb), it was tested at low carbosulfan concentration (10–22000 $\mu\text{g l}^{-1}$) using the optimum parameters, and the calibration curve was given in Fig. 1D as a log [carbosulfan] vs %I (percentage of inhibition), where the linear equation was $\%I = 0.223 \log [\text{carbosulfan}] + 0.0071$, with the correlation coefficient (r) value of 0.993. Based on this linear curve, the limit of detection (LOD) was calculated to be 10 $\mu\text{g l}^{-1}$. This LOD values was lower than previously reported work^{25,27} and allowed pesticide detection within the maximum pesticide residue (50 $\mu\text{g l}^{-1}$) allowed by the Indonesian Government.³⁰

Based on this calibration, the reproducibility for three consecutive days toward 100 $\mu\text{g l}^{-1}$ carbosulfan was found at 99.35 $\mu\text{g l}^{-1}$ with reproducibility was 5.17% (RSD), and this value fulfils the required reproducibility value (RSD <11%).³¹ While the recovery value (%) was found to be 91.79%, that meets the recovery value needed (80%–110%).³¹ While for interference studies, it was focused on the compound that presents in food sample that may interfere the biosensing, i.e., quercetin and amyllum, as they present at high concentration in the food sample, such as vegetables, and rice respectively. Herein, it was found that no interference from these compounds up to a ratio of 1: 100, since the interference was <5%. The biosensor lifetime can be used up to three days when it is stored at room temperature, as it retained 85% of its activity. It produces reproducible measurements for up to 1 month when it is stored in a chiller (4 °C) and up to two months when it is stored in cold storage (0 °C). Afterward, it gradually deteriorates due to the biosensor activity was reduced by more than 20% of its response.

Table I. Results of carbosulfan detection in the food samples between the LOT vs HPLC.

Sample	Lab on Tip ($\mu\text{g l}^{-1}$)	HPLC method ($\mu\text{g l}^{-1}$)
Lattice	980 ± 4.04	1010 ± 1.82
Cabbage	1330 ± 2.31	1368 ± 1.03
Tomato	510 ± 5.21	530 ± 1.04
Organic rice	870 ± 3.51	752 ± 1.05
Non-organic rice	710 ± 4.64	680 ± 1.20

The LOT applicability was tested toward vegetable samples and rice samples, then the results were compared with the HPLC as the reference method. The HPLC was performed using methanol as a solution, with acetonitrile: H₂O (80:20) as eluent using flow-rate at 1 ml min⁻¹ and UV detector at 275 nm.³² The samples were spiked with carbosulfan at five different concentrations, 500, 750, 1000, 1250, and 1500 $\mu\text{g l}^{-1}$, and the results are summarized in Table I with three replicate measurements. The linear regression analysis provided the correlation data indicates a good agreement between the two methods ($R^2 = 0.964$).


Summary

The use of a disposable pipette tip to create the novel approach of lab-on-a-tip has been developed. The proposed biosensor shows the compatibility of creating a novel one-shot optical fiber biosensor with simple operation. The simple procedure involves sample loading into the tip, and reacted 15 min as inhibition time, then added with the substrate. In this biosensing scheme, the indicator color change from blue to yellow will depend on the carbosulfan concentration as an inhibitor. The color change in the tip can be detected by fiber optic using a reflectance mode. The lab-on tip applicability can be used for other types of optical sensor membranes, such as PIM (polymeric inclusion membrane), etc., and various target analyte.

Acknowledgments

This work was supported by The Ministry of Research and Technology/BRIN, the Republic of Indonesia through the WCR Grant 2020.

ORCID

B. Kuswandi  <https://orcid.org/0000-0002-1983-6110>

References

- B. Kuswandi and R. Narayanaswamy, *Sensors Actuators, B Chem.*, **74**, 131 (2001).
- M. Atakay, Ö. Çelikbiçak, and B. Salih, *Anal. Chem.*, **84**, 2713 (2012).
- S. Cinti, V. Mazzaracchio, G. Öztürk, D. Moscone, and F. Arduini, *Anal. Chim. Acta*, **1029**, 1 (2018).
- B. Kuswandi, Nuriman, J. Huskens, and W. Verboom, *Anal. Chim. Acta*, **601**, 141 (2007).
- S. Chen and M. H. Shamsi, *J. Micromechanics Microengineering*, **27**, 083001 (2017).
- Q. Quan and Y. Zhang, *Nanobiomedicine*, **2**, 1 (2015).
- S. Ge, L. Zhang, and J. Yu, *Bioanalysis*, **7**, 633 (2015).
- Y. He, Y. Wu, J. Z. Fu, and W. Bin Wu, *RSC Adv.*, **5**, 78109 (2015).
- A. T. Singh, D. Lantigua, A. Meka, S. Taing, M. Pandher, and G. Camci-Unal, *Sensors (Switzerland)*, **18**, 1 (2018).
- H. I. A. S. Gomes and M. G. F. Sales, *Biosens. Bioelectron.*, **65**, 54 (2015).
- V. Onescu, D. O'Dell, and D. Erickson, *Lab Chip*, **13**, 3232 (2013).
- G. Rateni, P. Dario, F. Cavallo, G. Rateni, P. Dario, and F. Cavallo, *Sensors*, **17**, 1453 (2017).
- S. Liu, W. Su, and X. Ding, *Sensors (Basel)*, **16**, 2086 (2016).
- V. B. C. Lee, N. F. Mohd-Naim, E. Tamiya, and M. U. Ahmed, *Anal. Sci.*, **34**, 7 (2018).
- K. Yamada, D. Citterio, and C. S. Henry, *Lab Chip*, **18**, 1485 (2018).
- S. Altundemir, A. K. Uguz, and K. Ulgen, *Biomicrofluidics*, **11**, 041501 (2017).
- W. Khongpet, S. Pencharae, C. Puangpila, S. Krattap Hartwell, S. Lapanantnoppakhun, and J. Jakmunee, *Talanta*, **177**, 77 (2018).
- H. Lim, A. T. Jafry, and J. Lee, *Molecules*, **24**, 1 (2019).

19. J. Hou, G. Dong, Z. Tian, J. Lu, Q. Wang, S. Ai, and M. Wang, *Food Chem.*, **202**, 81 (2016).
20. N. Zhang, Y. Si, Z. Sun, S. Li, S. Li, Y. Lin, and H. Wang, *Analyst*, **139**, 4620 (2014).
21. R. Zhang, N. Li, J. Sun, and F. Gao, *J. Agric. Food Chem.*, **63**, 8947 (2015).
22. J. Deng, D. Lu, X. Zhang, G. Shi, and T. Zhou, *Environ. Pollut.*, **224**, 436 (2017).
23. A. Rianjanu, S. A. Hasanah, D. B. Nugroho, A. Kusumaatmaja, R. Roto, and K. Triyana, *Chemosensors*, **7**, 20 (2019).
24. M. A. Hidayat, W. Christiana, and B. Kuswandi, *Sens. Lett.*, **11**, 2207 (2013).
25. B. Kuswandi, C. I. Fikriyah, and A. A. Gani, *Talanta*, **74**, 613 (2008).
26. S. K. Park, C. T. Kim, J. W. Lee, O. H. Jhee, A. S. Om, J. S. Kang, and T. W. Moon, *Food Control*, **18**, 975 (2007).
27. M. E. I. Badawy and A. F. El-Aswad, *Int. J. Anal. Chem.*, 536823 (2014).
28. M. A. Hidayat, A. Fitri, and B. Kuswandi, *Acta Pharm. Sin. B*, **7**, 395 (2017).
29. B. Brogaard, K. Marlow, and K. Rice, *Rev. Philos. Psychol.*, **7**, 701 (2016).
30. A. Shoiful, H. Fujita, I. Watanabe, and K. Honda, *Chemosphere*, **90**, 1742 (2013).
31. L. Huber, *Validation and Qualification in Analytical Laboratories* (Informa Healthcare USA, Inc., New York, NY) 2nd ed. (2007).
32. US EPA, Analytical Methods and Procedures for Pesticides, <https://epa.gov/pesticide-analytical-methods>.

